2001-1504

A DOCKING SYSTEM FOR MICROSATELLITES BASED ON MEMS ACTUATOR ARRAYS*

David M. Meller
Joel Reiter, Mason Terry, Karl F. Böhringer, Ph.D., Mark Campbell, Ph.D
Department of Electrical Engineering
University of Washington
Seattle, WA 98195-2500

Abstract

Microelectromechanical system (MEMS) technology promises to improve performance of future spacecraft components while reducing mass, cost, and manufacture time. Arrays of microcilia actuators offer a lightweight alternative to conventional docking systems for miniature satellites. Instead of mechanical guiding structures, such a system uses a surface tiled with MEMS actuators to guide the satellite to its docking site.

This report summarizes work on an experimental system for precision docking of a "picosatellite" using MEMS cilia arrays. Microgravity is simulated with an aluminum puck on an airtable. A series of experiments is performed to characterize the cilia, with the goal to understand the influence of normal force, picosat mass, docking velocity, cilia frequency, interface material, and actuation strategy ("gait") on the performance of the MEMS docking system.

We demonstrate a $4cm^2$ cilia array capable of docking a 45g picosat with a $2cm^2$ contact area with micrometer precision. It is concluded that current MEMS cilia arrays are useful to position and align miniature satellites for docking to a support satellite.

Introduction

A number of MEMS cilia systems have been developed with the common goal of moving and positioning small objects, so far always under the force of gravity. Similar to biological cilia, all of these systems rely on many actuators working in concert to accomplish the common goal of transporting an object of much larger size than each individual cilium. Recent techniques range from air jets[1-3] electromagnetic actuators[4-6] piezoelectric actuators[7] single crystal silicon electrostatic actuators[8,9] thermal-bimorph (bimaterial) actuators[10-13] to electrothermal (single-material) actuators[14,15]. In parallel, researchers have studied the control of distributed microactuation systems and cilia arrays[16-22].

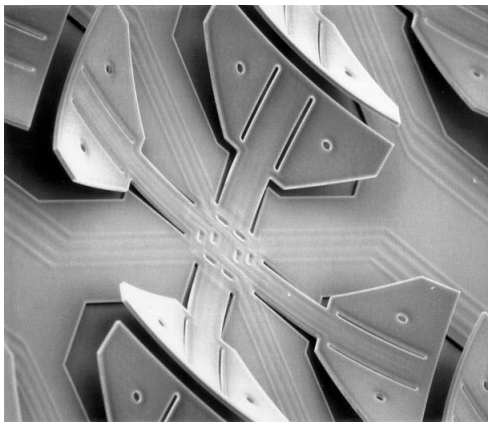

Figure 1. Scanning electron microscope (SEM) view of a single microcilia motion cell. The cell is approx. 1mm long and wide. (Image by John Suh, 1997)

The goal of this project was to investigate the feasibility of a MEMS-based space docking system. For such a system, the docking approach is divided into two phases: (1) free flight and rendezvous, with the goal to achieve physical contact between the two satellites, and (2) precision docking with the goal to reach accurate alignment between the satellites (e.g., to align electrical or optical interconnects). Phase 1 constitutes unconstrained motion with 6 degrees of freedom and lower accuracy for the rendezvous. Phase 2 constitutes planar motion with 3 degrees of freedom and high accuracy. The MEMS-based approach for phase 2 represents the key innovation in this project. Therefore, the investigation of MEMS cilia as a means to achieve precise alignment between two satellites represents the primary focus of this report. To demonstrate a complete system-level solution, phase 1 was investigated as well.

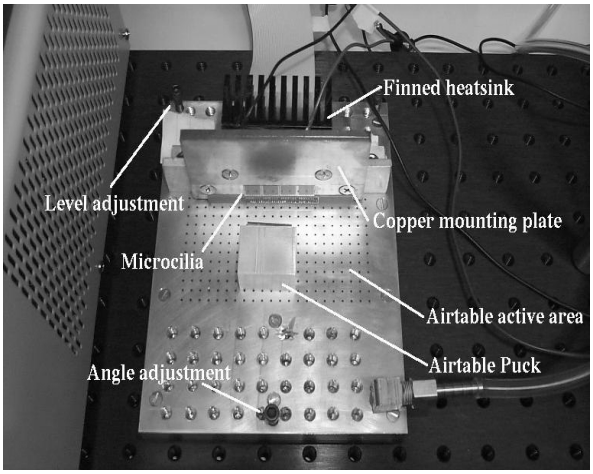

Figure 2. Airtable experimental setup to simulate microsatellite docking. An 8" × 6" perforated aluminum plate with 3 adjustable support screws provides levitation support for an aluminum puck ("picosat"). Microcilia chips are mounted on a vertical copper plate with heat sink.

During this project thermally actuated polyimide based microcilia, as seen in Figure 1 and identical to those published in Suh, et. al[13], are extensively characterized to ascertain their practicality for docking miniature spacecraft. To this end, experiments were performed using an airtable, seen in Figure 2, which was designed to support the microcilia in a vertical configuration. A rectangular aluminum block, referred to as a puck, which has a mass between 40g and 45g is used to simulate a picosatellite. The airtable can be tilted towards the microcilia producing a known normal force against the faces of the chips. This force can then be adjusted independently from the mass of the simulated picosatellite. To increase the realism of the experiment and to facilitate data collection, position sensing and position feedback are incorporated and computer controlled. Two position-sensing systems are used: an array of Hall effect sensors and a video capture based system. These are strictly non-contact techniques compatible with a space environment.

Next we describe the experiments that were performed with the microcilia with the goal to evaluate the appropriateness of microcilia to spacecraft docking applications. The microcilia successfully moved blocks of aluminum in excess of 40g of mass and calculations indicate that a patch of cilia 25cm in radius would be sufficient to position a 40kg satellite. Four different materials, polished ceramic, polystyrene, smooth aluminum and silicon, both rough and polished, are used for the cilia to puck interface surface. Polished ceramic achieved the highest puck velocities of all interfaces and polished silicon attained higher velocities than rough silicon. Throughout the course of this study microcilia were able to provide the speed, robustness, reliability and strength for use in miniature spacecraft applications.

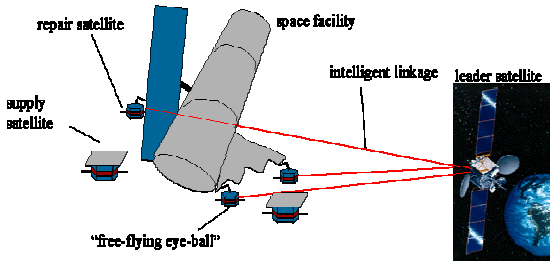

Figure 3. Envisioned microsatellite mission

Microsatellite Docking

Figure 3 describes a large, broad purpose satellite surrounded by a constellation of smaller, mission specific satellites. The miniature satellites provide inspection, maintenance, assembly and communication services for their larger brethren. One important future task for the microsatellites is inspecting the larger satellite for damage. Cameras mounted on the microsatellite provide imagery of the primary platform that is otherwise unobtainable. From these pictures, damage could be assessed and the mission of the main satellite adapted. Due to their simplicity, small size, weight and limited interaction with ground controllers these specialized satellites are expected to be indispensable during future missions[23].

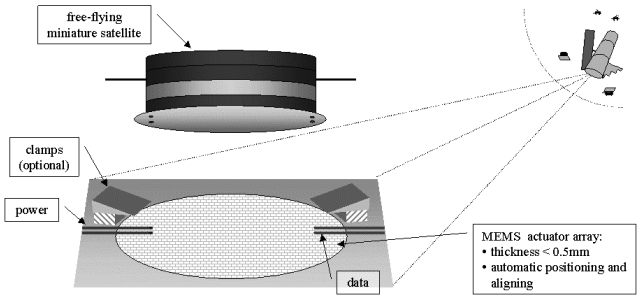

Figure 4. Conceptual cilia picosatellite docking application

As the size of satellites shrink, their ability to carry fuel and power is reduced. It is expected that this will force microsatellites to dock frequently to replenish their resources. Since the time spent docking subtracts from the microsatellites' mission time, this procedure should be as simple and quick as possible. When docking microspacecraft there are two primary tasks: attaching the microsatellite to the larger craft, and orienting the satellite to connect fuel, data and electrical services. The first docking task is largely the domain of the microsatellite and is dependent on how quickly

velocity adjustments can be made, and on the specific attachment mechanism. The second phase of docking is dependent on the speed at which the satellite can be positioned to connect electrical and other services.

Figure 4 shows the conceptual cilia application for space docking of miniature satellites. A surface on the mother satellite is covered with cilia actuators that will position the picosatellite for refueling and data transfer.

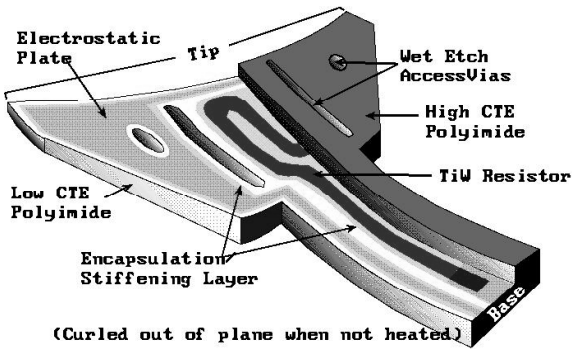

Figure 5. Cross-sectional view of the cilia with two layers of polyimide, titanium-tungsten heater loop, silicon-nitride stiffening layer, and aluminum electrostatic plate. (Image by John Suh, 1997)

Experimental Setup

The measurements in this paper are performed using the thermal actuator based microcilia originally described in Suh, et. al[13]. A cross-section of microcilia arms is shown in Figure 5. The arrayed actuators are deformable microstructures that curl out of the substrate plane. The curling of the actuators is due to the different CTE of the polyimide layers that make up the bimorph structures. For these devices the top layer CTE is greater than the bottom CTE. The thermal stress from this interface causes the actuator to curl away from the substrate at low temperatures and towards it when heated. This stress also aids in releasing the microcilia arms because they automatically rise out of the plane when the sacrificial layer is etched. The displacement of the microcilia arm relative to its location before release both vertically, δ_V, and horizontally, δ_H, is given by:

$$\delta_V = R\left(1-\cos\left(\frac{L}{R}\right)\right) \quad (1)$$

$$\delta_H = L - R\sin\left(\frac{L}{R}\right) \quad (2)$$

where R (≈ 800μm) is the radius of curvature and L (≈ 430μm) is the length of the motion actuator which results in a horizontal displacement, δ_H, of 20μm and vertical displacement, δ_V, of 114μm. A detailed description of the cilia actuators and their operation was presented in Suh, et. al[12,13].

An array of cilia is configured in an 8 × 8 motion cell layout within a 1cm^2 die. Each motion cell contains four orthogonally-oriented actuators within an area of 1.1mm × 1.1mm. A control line independently actuates each actuator of the motion cell. All actuators oriented in the same direction in each motion cell are controlled in parallel.

The microcilia arm is placed into motion using a titanium-tungsten heating resistor that is sandwiched between the two silicon nitride and two polyimide layers. When a current is passed through this loop, the temperature of the actuator increases, and the structure deflects downward. This produces both horizontal and vertical displacements at the tip of the microcilia.

Objects in contact with the surface of the array are made to move by coordinating the deflections of many actuators. For this study both three and four-phase gaits are used during the interface experiments but only the four-phase gait is used for the normal force experiments. The motions of the microcilia arms for the four-phase gait are shown in Figure 6. This motion has two transitions that produce forward motion.

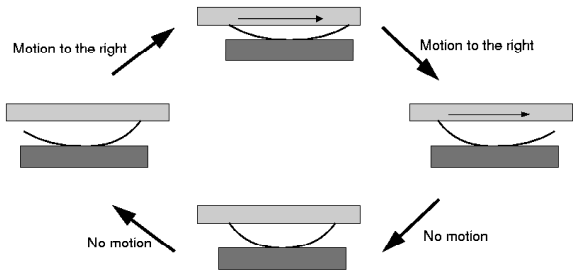

Figure 6. The four phase cilia motion gait showing all phases of motion

The sequence of phases starts with both arms flattened. The west arm is released forcing the object up and to the east. Next, the east arm is released which rises to make contact with the object. Then the west arm is actuated leaving the east actuator to support the object. The final phase and start of a new phase in the sequence results in the object moving down and to the east. The three phase gait is the same as the four phase except the phase in top of Figure 6 is skipped.

To assess the applicability of microcilia to spacecraft docking this study investigates the effects of: operating frequency, normal force, interface surfaces, microcilia temperature, and, indirectly, microcilia life

span. Of these variables, frequency and life span depend directly on the thermal actuation nature of the cilia while the remaining parameters should be applicable to other types of MEMS microactuator arrays.

To perform measurements the microcilia are placed vertically, at the end of a tilted airtable as show in Figure 7. The table is first leveled and then the angle adjustment is manipulated to specify a slope running towards the microcilia. By adjusting the slope of the table, the mass of the aluminum airtable puck can vary while the normal force against the microcilia remains constant. Conversely, the mass can remain fixed while a variable normal force is applied against the microcilia. Using this parameter independence, the airtable allows for an accurate simulation of microsatellite docking in microgravity.

With this setup, the microcilia can manipulate objects that would otherwise flatten the actuators if all the gravitational force were applied as the normal force. This experiment uses four microcilia chips attached to a copper block that both actively cools the microcilia using a Peltier junction and holds them vertical at the end of the airtable. The microcilia chips were glued into a grove machined in the copper block, forcing all four chips to lie in the same plane in a horizontal linear array.

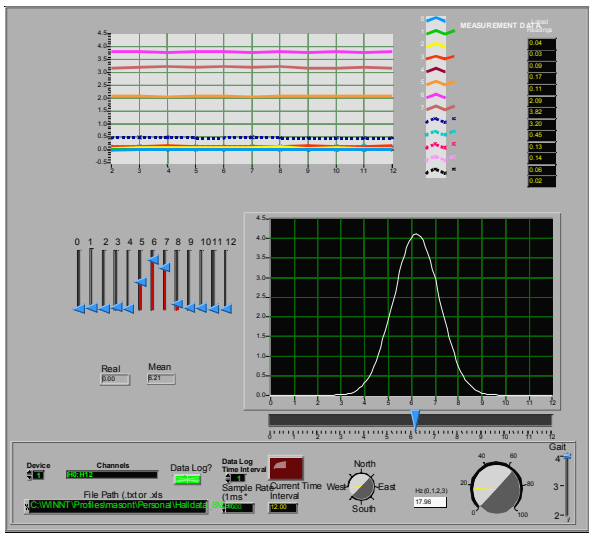

Figure 7. LabView interface for the microcilia

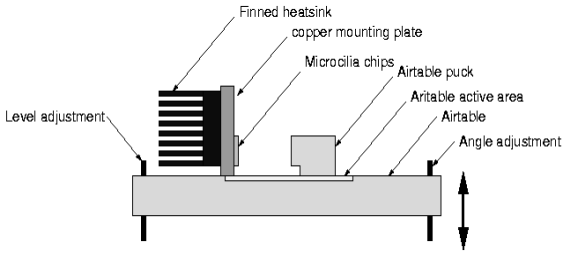

Figure 8. Side view of the airtable

During all of the experiments the microcilia were controlled with the LabView interface seen in Figure 7 and custom circuitry. Each of the microcilia gaits is broken down into a statemachine describing the sequence of movements for each of the microcilia arms. This statemachine is then loaded into a LSI programmable gate array, one per microcilia chip. The LabView interface instructs the LSI chips which gait to use, the direction to travel and the frequency through which to cycle the cilia gait. LabView also reads the Hall effect sensor array and from that data controls the starting and ending points of the puck.

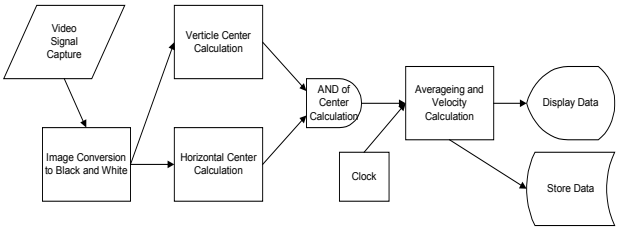

Figure 9. Block flow diagram of image capture system

To make displacement measurements two separate systems are employed. The first is a high-resolution video capture system. This system, equipped with a zoom lens, allows for relative measurements on the order of 5μm and for capturing expanded views of the system. A video capture and distance measurement system has been developed. A flow diagram, shown in Figure 9, details the specific tasks that are performed upon a video image. The image of the puck is captured using a black and white CCD camera mounted on a variable zoom, 1-10, microscope. This image is then converted to a black and white image to allow processing using Matlab.

Once converted, the center points of both the horizontal and vertical white regions are calculated. After the center point calculations are complete, Matlab performs an AND function to determine the center pixel of the captured image. All of the center points can be combined and averaged relative to an internal clock to reduce the error of the capture system.

The other measurement system is an array of Hall effect sensors. These sensors interact with a magnet mounted atop the puck to provide micrometer resolution. The Hall effect sensor array is integrated into the LabView controlling software allowing fully automated experiments to be performed. Using either of these systems it is possible to collect relative puck position and from this to compute the velocity and acceleration of the puck.

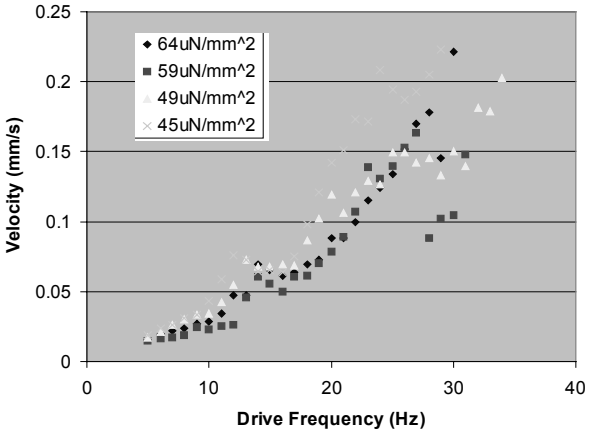

Figure 10. The velocity of the airtable puck (using the beveled plastic interface) versus different drive frequencies as a function of normal forces

Experimental Results

The goal of this research is to evaluate the applicability of microcilia arrays to microsatellite docking. Thermal microcilia arrays are parameterized for operating frequency, normal force, puck mass, interface surfaces, cilia temperature and cilia lifespan. The results for these experiments are presented here.

Effects of Normal Force

Figure 10 shows the velocity of the puck at different frequencies for four different normal forces. For all of these data points the mass of the puck is 41.20gr and the interface surface is a 0.9cm × 2.5cm piece of polystyrene, beveled on the edges. Each data point is an average of four runs over a distance of 0.8mm. This setup contains two strong resonant frequencies between 13 and 16Hz and between 30 and 33Hz as illustrated by the graph flattening at these points. For these measurements the video system is used to record the puck velocity.

Outside of these regions the puck velocity increases linearly which indicates the puck moving in accordance to the driving period. This characteristic indicates the interface between the puck and microcilia arms is experiencing a fixed slip component. At these frequencies the puck motion seems largely the result of a 'step and carry' transport. One conclusion from this graph is that the overall velocity of the puck increases as the normal force against the cilia surface decreases to a minimum normal force value. This is an expected result because as the normal force increases so does the precompression of the cilia, reducing their total vertical and horizontal motion. This would indicate that the optimal normal force is that where the puck exerts just sufficient force to maintain contact with the cilia surface.

Effects of Interfacing Surfaces

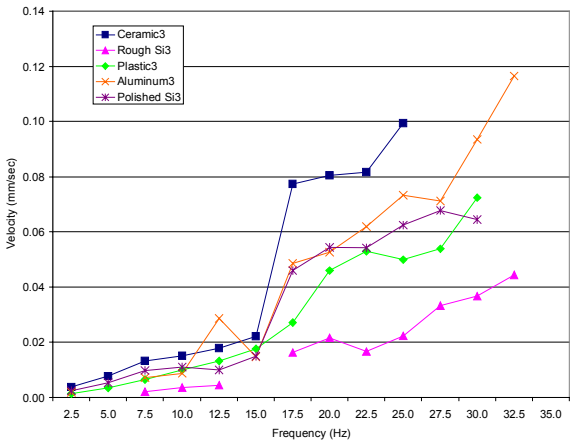

Figure 11. Influence of interface material on puck velocity using a three-phase gait

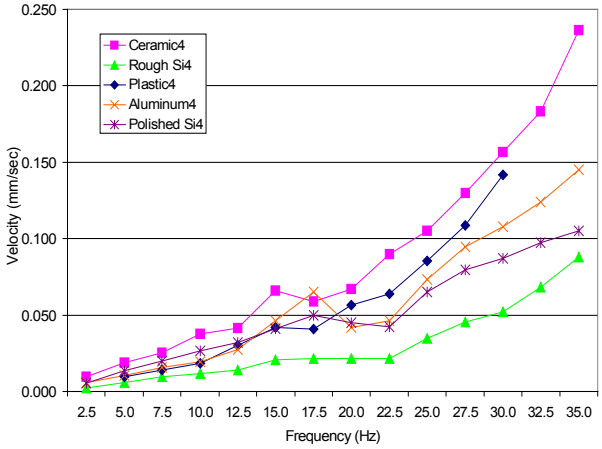

Figure 12. Influence of interface material on puck velocity using a four-phase gait

Differences between thermal conduction and surface roughness of the puck to microcilia interface affect step size and puck velocity. The five puck-to - microcilia interface materials examined are: polished ceramic, hard polystyrene plastic, aluminum, polished

and unpolished silicon. Puck velocity versus frequency for the differing interface materials is shown in Figure 11 and Figure 12 for three and four-phase gaits, respectively. Puck velocity is obtained by averaging a minimum of five trials per frequency with a normal force of 63μN/mm^2. The distance the puck traveled for these measurements varies between 0.1mm to 0.6mm with increasing actuation frequency.

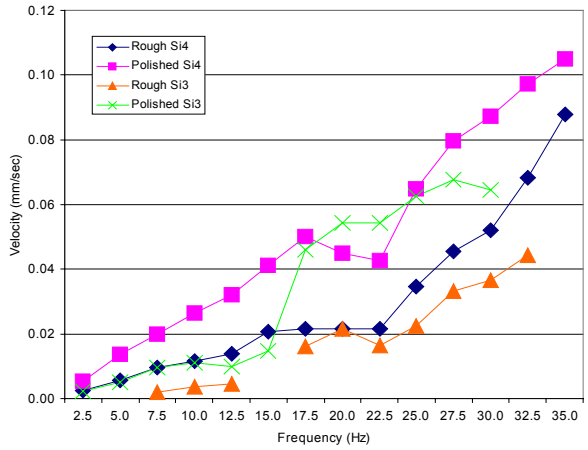

Figure 13. Comparison of both rough and polished silicon interface for both three and four-phase gaits

As summarized in Figure 13, the velocity of the puck is dependent on the material interfaced with the microcilia. The thermal conduction of the interface material is thought to be the major cause for the variation in velocity magnitude per material. Surface roughness is also observed to have some influence, but to a much lesser extent. Aluminum and silicon have the highest thermal conduction and this results in the lowest velocities. Ceramic, an excellent thermal and electrical insulator, delivers some of the highest velocities. Low thermal conduction of the ceramic interface allows the cilia to heat and cool in an optimal fashion resulting in high actuation amplitudes and high velocities.

Missing data points in the three-phase graph and the flatter areas of the other graphs are due to the puck oscillating with zero or reduced velocity for multiple trials at that frequency. This effect is distributed over the entire cilia experimental surface. The regions of 17.5Hz and 33Hz show the most pronounced reduction in puck velocity for both gaits and all interface materials. The variation of this effect for different surface material and puck mass indicates that it is strongly dependent upon the specific geometry of the experiment. Regardless of this minor variation, it is thought that this phenomenon can be traced partly to the puck breaking contact with the microcilia surface during part of the motion cycle. As the normal force is increased, this effect becomes less pronounced, however, it is still consistently observed. Within these frequency bands the puck was observed to move away from the puck surface on the order of 100μm, lending support to this theory.

Thermal Effects

As the background temperature of the microcilia is allowed to increase the actuators become less effective. With rising background temperature it takes longer for the cilia to gain heat during the actuated portion of its motion cycle. This results in a lowering of the maximum available driving frequency. In the extreme case the background temperature becomes large enough that the heater loop cannot raise the temperature of the cilia higher than the background. At this background temperature, no heating period would be sufficient to allow the cilia to have a net displacement. At this point, objects in contact with the cilia would no longer be transported.

This scenario was experimentally verified. If the polarity of the Peltier junction that normally cools the microcilia is reversed, it provides active heating, rather than active cooling. As the background temperature of the cilia increases, actuation displacement decreases. Eventually all visible movement halts. Once this point is reached the heater is turned off and the microcilia are allowed to cool. Subsequent checks of the microcilia, under standard operating conditions, could determine no mechanical or electrical faults. However, prolonged operation at elevated temperatures will eventually damage the actuators. Possible failures include charring of the polyimide and fusing of the heater wire.

Life Span

Over the course of these experiments the microcilia are shown to be robust and the results reproducible. All four chips, corresponding to 4 × 256 actuators were run for approximately 150 hours at an average of 20Hz. This corresponds to 10.8 million actuations. During this time only one microcilia actuator leaf was lost due to a manufacturing defect. This failure was in an individual heater loop and probably corresponded to a local thickening of the material or contaminants in that area.

Novel Algorithms and Control Software

Rendezvous & Docking

Numerous studies have been made in the area of Rendezvous and Docking (R&D) of small satellites in space. These studies generally involve small “satellite” robot vehicles moving in 2 nearly frictionless degrees of freedom on an air-bearing surface. Two primary approaches have traditionally been pursued. The first

of these approaches is the use of GPS-like signals and Differential Carrier Phase GPS techniques as a means of sensing both the relative position and the relative attitude of the two satellites. An example can be found in Zimmerman and Cannon, Jr.[25] To simulate the GPS environment, several pseudolite transmitters were built and installed around the perimeter of a laboratory. Algorithms were then developed to extract relative position and relative attitude from carrier phase measurements.

The second primary approach has been the use of CCD, or camera-based sensing to determine relative positions and attitudes between the sensor and the target. An example of this approach can be found in Howard and Book[26]. This study, performed at NASA's Marshall Space Flight Center, employed a single CCD sensor and laser diodes to illuminate a target. The images were then processed to determine navigation data. This approach has been further developed by NASA and is currently being built as a prototype for flight testing on the Space Shuttle. An important point to note in this approach is the use of analog CCD sensors and frame-grabber hardware for target sensing.

2-D Puck Experiment

Experimental Approach

The approach to R&D presented in this section is a variation of the approach taken by Howard and Book, that is, the use of optical sensing and image processing to determine relative navigation data. However, this approach differs significantly from the work cited above. Sensing is provided by two 512 × 512 Fuga 15d digital CMOS cameras. The two cameras are mounted parallel to one another, separated by a baseline distance. In this configuration the cameras can determine range and attitude with respect to a target through stereo imaging. Another significant difference is the absence of frame-grabber hardware for image capture, since the cameras feature digital output.

The Fuga 15d Digital CMOS Camera

The use of digital, optical, CMOS cameras offers many advantages over analog CCD cameras. The Fuga 15d, from the IMEC Company, is a 512×512 pixel, addressable imaging chip that behaves similar to a 256 Kbyte ROM. After reading an *X-Y* address, the pixel intensity is directly read out and returned in a digital word of 8 bits, allowing true random access. Direct readout means that the output signal is an instantaneous measure of the photocurrent. Camera response is logarithmic, which allows the chip to capture six or more orders of magnitude of intensities in the same image. As a result, the sensor is virtually immune to blooming. The camera can take a picture of a welding arc without saturating. The Fuga 15d camera is shown in Figure 14.

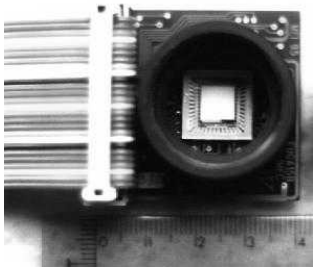

Figure 14. The Fuga 15d Digital CMOS Camera

Direct readout and random access are a substantial advantage over analog imagers. Classic CCD and even addressable Metal-Oxide-Semiconductor (MOS) imagers of the "integrating" type must be read out after a defined integration time, and thus cannot be used as true random access devices. Analog cameras also require frame grabber hardware, whereas the full matrix of pixels, or any desired pixels, on the Fuga 15d can be simply scanned and read directly into a buffer.

Pixel data is read from the camera ROM through 8 parallel, digital output lines. Image processing algorithms must use the intensity value corresponding to each pixel to determine the target location in each camera image. A hardware solution was adopted to handle image processing and data flow using an FPGA. Output lines from the cameras are mapped directly to the hardware, and all image processing analysis is carried out by the FPGA processor.

Stereo Imaging

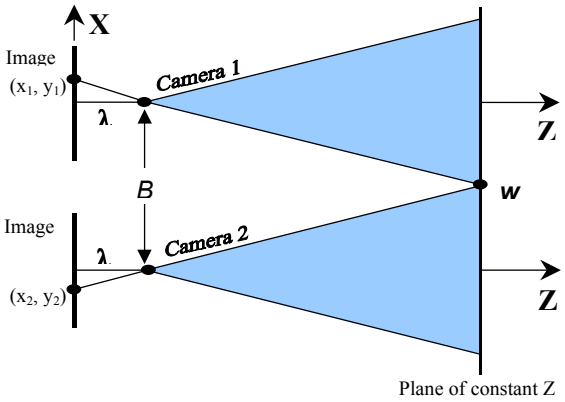

Figure 15. Top view of the stereo imaging process (From Fu, Gonzalez and Lee[28].)

Much as in human vision, two cameras imaging the same target can provide sufficient information about the orientation and location of the target[27]. The process of

mapping a 3D scene onto an image plane is a many-to-one operation. This means that a single image point does not uniquely determine the location of a corresponding point in the 3-dimensional world. More precisely, the *range* to a target cannot be accurately determined from a single camera image. The missing range information can be determined using stereo imaging techniques.

The objective, stated in another way, is to find the coordinates (X,Y,Z) of the point w given its image points (x_1, y_1) and (x_2, y_2). It is assumed that the cameras are identical and that the coordinate systems of both cameras are perfectly aligned, differing only in the locations of their origins, which are separated by the baseline distance, B. Range information determined by the x-coordinate shift of the target location in each camera image, or the quantity (x_2-x_1), using the following equation:

$$Z = \lambda - \frac{\lambda B}{x_2 - x_1} \tag{3}$$

The most challenging task in implementing the stereo imaging approach is to accurately determine two corresponding points in two different images of the same scene. However, with proper target design and image processing techniques, this can be reliably accomplished. For example, the image might consist of a series of concentric circles against a highly contrasting background. A simple algorithm could then be developed to determine the pixel center of the binarized image and, therefore, the target center.

The 2-D Puck

A 2-dimensional experiment has been developed that will serve as a test bed for integration of sensors and for verification of control algorithms. The 2-D "Puck" consists of a series of vertically stacked decks, floating upon a low-friction cushion of air supplied by an on-board air system. The cameras are mounted near the outer edge of the second deck and integrated electronically to a central computer. Control is accomplished with small solenoid valves that act as air thrusters. Eight thrusters are placed around the circumference of the second deck, enabling control in the $\pm x$, $\pm y$ directions and spin control about the vertical axis. When placed on a sufficiently flat surface the puck can translate in two dimensions and rotate about its spin axis with very little friction. The goal of the experiment is to electronically integrate and close the loop with the CMOS sensors and to demonstrate rendezvous with a stationary target.

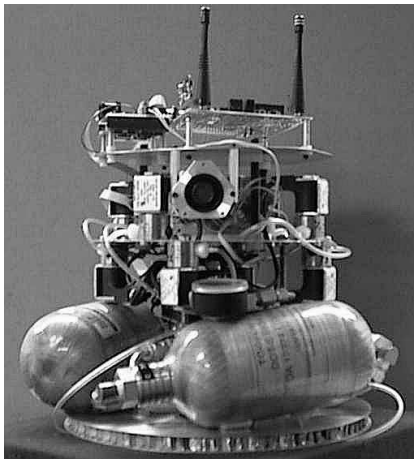

Figure 16. 2-D Puck Experiment with integrated CMOS camera

All sensor measurements are sent to a TattleTale 8 controller board (TT8), which includes a Motorola 68332 microprocessor, a 500 Kbaud RS-232 interface and a PIC 16C64 microcontroller operating as a super-programmable clock. Data processing software and control algorithms are loaded into the EEPROM of the 68332 microprocessor. The TT8 processes incoming sensor signals and sends control signals to the solenoid valves, thus closing the loop.

Puck Control and Navigation – An Augmented Approach

While the puck is capable of fully autonomous navigation to accomplish rendezvous with the cilia array, an augmented navigation and control approach is more desirable. The puck will follow a predetermined reference trajectory, passing through a waypoint. This strategy is to ensure that the final approach and contact with the cilia is as perpendicular to the plane of the cilia as can realistically be achieved with the control system of the puck. This requirement is especially important to avoid damage to the cilia arrays caused by a rendezvous with lateral motion components, i.e., in the plane of the cilia array. Such an interaction between the puck and array could tear and damage the cilia actuators. An illustration of the waypoint trajectory can be seen below in Figure 17. The initial navigation phase sends the puck to the waypoint, which is somewhere removed from the final destination. The next phase directs the puck to slowly approach the cilia array, holding the lateral (X) coordinate constant.

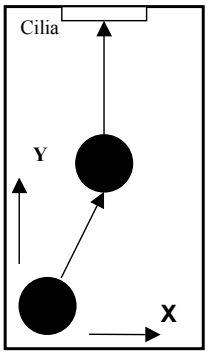

Figure 17. Table schematic and puck trajectory

The dynamics of the puck were modeled and included in a discrete-time simulation with LQR control using the reference trajectories. Both the reference and simulated paths are shown in Figure 18. In the lower curve, the ideal x trajectory ramps up to the desired value, corresponding to the waypoint, and subsequently remains constant. The y coordinate ramps up to the waypoint coordinate and from that point follows a slowly increasing parabolic input to slowly approach the final position at the cilia array. The simulation closely tracked the reference trajectory and final position using LQR control.

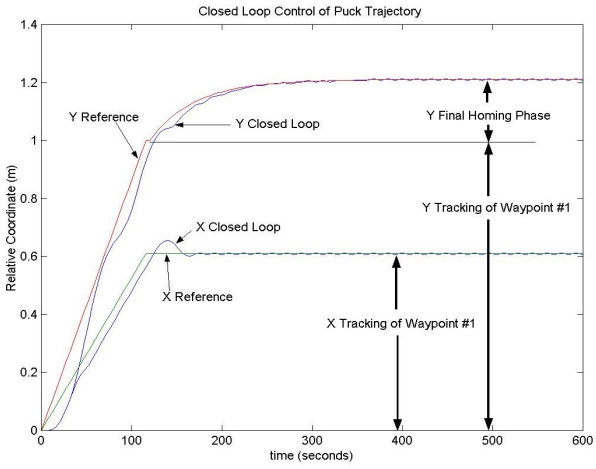

Figure 18. Closed loop response to reference trajectory using LQR control.

Conclusions

The results from these experiments indicate that a microcilia surface can be useful for docking small spacecraft. These spacecraft, used for inspection, maintenance, assembly and communication services, will see increased use as space missions become more autonomous and far reaching[23]. During this scenario, microcilia provide a good match, allowing for simple docking procedures to be used with these simple satellites.

Results from the interface experiments indicate that a variety of materials common to spacecraft can be used as docking surfaces, including aluminum and silicon, thus avoiding the need for special materials on the mating surfaces. When studying the performance of different interface materials, thermal conduction dominates surface roughness to achieve optimal object velocity. Surface roughness does affect object velocity as seen in the polished and unpolished silicon. An interface material, such as ceramic, with low thermal conduction and little surface roughness should be selected for an optimal docking surface.

Using microcilia to perform the delicate final orientation and positioning of the satellite will greatly speed up the docking operation because the entire satellite, with its fixed connections, could be mated to fixed connections on the main satellite. This alleviates the use of flexible and cumbersome umbilical cords and attendant positioning systems.

A further benefit of using microcilia as a docking surface is a reduction in mass compared to other docking and alignment techniques. On the host satellite only a surface of microcilia is required along with minimal control electronics and sensors. The microcilia docking system could simply replace one of the satellite's body panels for maximum weight savings. On the microsatellite side, the additional mass to incorporate docking functionality could be as low as zero. The optimal microcilia interface is a flat plane, which may already be part of the microsatellite chassis, thus requiring minimal integration.

The microcilia themselves have inherent advantages for this application. Foremost among these advantages is their ability to arbitrarily position the satellite anywhere on the surface and in any orientation. The microcilia can also act as sensors, however, it has already been demonstrated that they can position objects open loop with little loss of accuracy[18]. By using thousands of microcilia on a single docking patch, it is possible to build systems that incorporate massive redundancy. Thus, if there is some kind of docking mishap the entire mission need not be affected. Finally, thermal microcilia have been shown to perform better in vacuum then air[24]. This is largely due to a lack of convective cooling which slows the heating cycle.

The scalability of microcilia also enables the construction of widely varied systems. While the primary task envisioned for microcilia is manipulating picosatellites (mass <1kg) much greater masses are feasible. By using additional cilia and a greater contact area, larger microsatellites can be handled. The current

generation of microcilia is capable of moving a 41.2g puck with an interface area of $2cm^2$. This indicates that a patch only 25cm in radius (100,000 times as large as the area in the experiment) would be sufficient to position satellites with more than 40kg mass under microgravity conditions.

Throughout the course of this study the microcilia exhibited the speed, robustness, reliability and strength needed for this application. These results show that microcilia can be an attractive alternative to conventional docking systems for microsatellite applications.

Acknowledgments

This report describes work on "Smart Attachments" performed under AFRL prime contract F29601-98-D-0210, USRA subcontract 9500-20, 8/24/99 - 8/23/00. Team members were Dr. Karl F. Böhringer (PI), Department of Electrical Engineering, and Dr. Mark Campbell (co-PI), Department of Aeronautics and Astronautics, University of Washington, Seattle, WA. Joel Reiter, Mason Terry (UW EE), and David M. Meller (UW AA) were graduate students working on this project. Dr. R. Bruce Darling (UW EE), Dr. Gregory T. A. Kovacs (Department of Electrical Engineering, Stanford University, CA), and Dr. John W. Suh (Xerox Palo Alto Research Center, CA) were informal consultants.

The authors wish to thank Mike Sinclair for the manufacture of the airtable setup and for many inspiring discussions. We are grateful to the members of the University of Washington MEMS Laboratory, and the members and staff of the Washington Technology Center Microfabrication Laboratory. Fabrication of the microcilia arrays was supported by DARPA and NSF. Development of cilia control strategies was supported by NSF.

References

1. K. S. J. Pister, R. Fearing, and R. Howe, "A planar air levitated electrostatic actuator system," in *Proc. IEEE 5th Workshop on Micro Electro Mechanical System*s, Napa Valley, CA, Feb. 1990, pp. 67–71.
2. S. Konishi and H. Fujita, "A conveyance system using air flow based on the concept of distributed micro motion systems," *J. Microelectromech. Syst*., vol. 3, no. 2, 1994, pp. 54–58.
3. Y. Mita, S. Konishi, and H. Fujita, "Two dimensional micro conveyance system with through holes for electrical and fluidic interconnection," in *Transducers '97 Dig. 9th Int. Conf. on Solid-State Sensors and Actuator*s, vol. 1, Chicago, IL, June 16–19, 1997, pp. 37–40.
4. C. Liu, T. Tsai, Y.-C. Tai, W. Liu, P. Will, and C.-M. Ho, "A micromachined permalloy magnetic actuator array for micro robotics assembly systems," in *Transducers '95 Dig. 8th Int. Conf. on Solid-State Sensors and Actuators/Eurosensors I*X, vol. 1, Stockholm, Sweden, June 1995, pp. 328–331.
5. W. Liu and P. Will, "Parts manipulation on an intelligent motion surface," in *Proc. 1995 IEEE/RSJ Int. Conf. on Intelligent Robots and System*s, Pittsburg, PA, vol. 3, Aug. 5–9, 1995, pp. 399–404.
6. H. Nakazawa, Y. Watanabe, and O. Morita, "The two-dimensional micro conveyor: Principles and fabrication process of the actuator," in *Transducers '97 Dig. 9th Int. Conf. on Solid-State Sensors and Actuator*s, vol. 1, Chicago, IL, June 16–19 1997, pp. 33–36.
7. T. Furihata, T. Hirano, and H. Fujita, "Array-driven ultrasonic microactuators," in *Transducers '91 Dig. 6th Int. Conf. on Solid State Sensors and Actuator*s, San Francisco, CA, June 1991, pp. 1056–1059.
8. K.-F. Böhringer, B. R. Donald, and N. C. MacDonald, "Single-crystal silicon actuator arrays for micro manipulation tasks," in *Proc. IEEE 9th Workshop on Micro Electro Mechanical Systems (MEMS*), San Diego, CA, Feb. 1996, pp. 7–12.
9. K.-F. Böhringer, B. R. Donald, N. C. MacDonald, "Programmable Vector Fields for Distributed Manipulation, with Applications to MEMS Actuator Arrays and Vibratory Parts Feeders." *International Journal of Robotics Research,* 18(2):168-200, February 1999.
10. N. Takeshima and H. Fujita, "Polyimide bimorph actuators for a ciliary motion system," in *ASME WAM, Symp. Micromech. Sensors, Actuators, and System*s, DSC-vol. 32, 1991, pp. 203–209.
11. M. Ataka, A. Omodaka, and H. Fujita, "A biomimetic micro motion system," in *Transducers '93 Dig. 7th Int. Conf. on Solid State Sensors and Actuator*s, Pacifico, Yokohama, Japan, June 1993, pp. 38–41.
12. J. W. Suh, S. F. Glander, R. B. Darling, C. W. Storment, and G. T. A. Kovacs, "Combined organic thermal and electrostatic omnidirectional ciliary microactuator array for object positioning and inspection," in *Tech. Dig. Solid-State Sensors and Actuator Worksho*p, Hilton Head, SC, June 1996, pp. 168–173.
13. J. W. Suh, S. F. Glander, R. B. Darling, C. W. Storment, and G. T. A. Kovacs, "Organic thermal and electrostatic ciliary microactuator array for

object manipulation," *Sensors and Actuators, A: Physica*l, vol. A58, 1997, pp. 51–60.
14. T. Ebefors, J. U. Mattsson, E. Kèlvesten, and G. Stemme, "A robust micro conveyor realized by arrayed polyimide joint actuators," in *Proc. IEEE 12th Workshop on Micro Electro Mechanical Systems (MEMS*), Orlando, FL, Jan. 1999, pp. 576–581.
15. P. E. Kladitis, V. M. Bright, K. F. Harsh, and Y. C. Lee, "Prototype microrobotics for micro positioning in a manufacturing process and micro unmanned vehicles," in *Proc. IEEE 12th Workshop on Micro Electro Mechanical Systems (MEMS*), Orlando, FL, Jan. 1999, pp. 570–575.
16. H. Fujita, "Group work of microactuators," in *Int. Adv. Robot Program Workshop on Micromachined Technologies and System*s, Tokyo, Japan, Oct. 1993, pp. 24–31.
17. Böhringer, K., Donald, B., Mihailovich, R., MacDonald, N.C., 1994, "A Theory of Manipulation and Control for Microfabricated Actuator Arrays," *Proceedings, IEEE MEMS '94,* pp. 102-104.
18. W. Liu and P. Will, "Part manipulation on an intelligent motion surface," in *IEEE/RSJ Int. Workshop on Intelligent Robots & Systems (IROS*), vol. 3, Pittsburg, PA, Aug. 1995, pp. 399–404.
19. Böhringer, K., Suh, J., Donald, B., Kovacs, G., 1997, "Vector fields for task-level distributed manipulation: experiments with organic micro actuator arrays," *Proceedings, 1997 IEEE International Conference on Robotics and Automation,* vol. 2, pp. 1779-1786.
20. K.-F. Böhringer, B. R. Donald, N. C. MacDonald, "Programmable Vector Fields for Distributed Manipulation, with Applications to MEMS Actuator Arrays and Vibratory Parts Feeders." *International Journal of Robotics Research*, 18(2):168-200, February 1999.
21. Mita, Y., Kaiser, A., Stefanelli, B., Garda, P.; Milgram, M., Fujita, H., 1999, "A distributed microactuator conveyance system with integrated controller," *Proceedings, IEEE SMC '99,* vol.1, pp. 18–21.
22. K.-F. Böhringer and Howie Choset, *Distributed Manipulation,* Kluwer Academic Publishers, 272 pp., ISBN 0-7923-7728-1, January 2000.
23. Campbell, M., Böhringer, K., 1999, "Intelligent Satellite Teams for Space Systems," *Proceedings, 2nd Int. Conf. on Integrated Micro/Nanotechnology for Space Applications,* vol. 2, pp. 193-204.
24. Darling, R., Suh, J., Kovacs, G., 1998, "Ciliary Microactuatory Array for Scanning Electron Microscope Positioning Stage," J. Vac. Sci. Tech. A, vol. 16, no. 3, pp. 1998-2002, May/Jun.
25. Zimmerman, K. R. and Cannon, Jr., R. H., "Experimental Demonstration of GPS for Rendezvous Between Two Prototype Space Vehicles." In *Proceedings of the 8th International Technical Meeting of the Satellite Division of the Institute of Navigation*, Palm Springs, CA, Sept. 12-15, 1995. Pt. 2 (A96-15026 02-17), Alexandria, VA, Institute of Navigation, 1995, p. 1905-1913.
26. Howard, Richard T. and Book, Michael L. "Improved Video Guidance Sensor for Automated Docking." In *Space guidance, control and tracking II; Proceedings of the Third Conference*, Orlando, FL, Apr. 17, 18, 1995 (A95-37727 10-19), Bellingham, WA, Society of Photo-Optical Instrumentation Engineers (SPIE Proceedings. Vol. 2466), 1995, p. 118-127.
27. Gonzalez, Rafael C. *Digital Image Processing*. Addison-Wesley Publishing Company, Inc., 1987.
28. Fu, K. S., Gonzalez, R. C., and Lee, C. S. G., 1987. *Robotics: Control, Sensing, Vision and Intelligence,* McGraw-Hill, New York.